

# Integration of Multiple Nutrient Cues and Regulation of Lifespan by Ribosomal Transcription Factor *Ifh1*

Ling Cai,<sup>1</sup> Mark A. McCormick,<sup>2</sup> Brian K. Kennedy,<sup>2</sup> and Benjamin P. Tu<sup>1,\*</sup>

<sup>1</sup>Department of Biochemistry, UT Southwestern Medical Center, 5323 Harry Hines Boulevard, Dallas, TX 75390-9038, USA

<sup>2</sup>Buck Institute for Research on Aging, 8001 Redwood Boulevard, Novato, CA 94945, USA

\*Correspondence: [benjamin.tu@utsouthwestern.edu](mailto:benjamin.tu@utsouthwestern.edu)

<http://dx.doi.org/10.1016/j.celrep.2013.08.016>

This is an open-access article distributed under the terms of the Creative Commons Attribution-NonCommercial-No Derivative Works License, which permits non-commercial use, distribution, and reproduction in any medium, provided the original author and source are credited.

## SUMMARY

Ribosome biogenesis requires an enormous commitment of energy and resources in growing cells. In budding yeast, the transcriptional coactivator *Ifh1p* is an essential regulator of ribosomal protein (RP) gene transcription. Here, we report that *Ifh1p* is dynamically acetylated and phosphorylated as a function of the growth state of cells. *Ifh1p* is acetylated at numerous sites in its N-terminal region by *Gcn5p* and deacetylated by NAD<sup>+</sup>-dependent deacetylases of the sirtuin family. Acetylation of *Ifh1p* is responsive to intracellular acetyl-CoA levels and serves to regulate the stability of *Ifh1p*. The phosphorylation of *Ifh1p* is mediated by protein kinase A and is dependent on TORC1 signaling. Thus, multiple nutrient-sensing mechanisms converge on *Ifh1p*. However, instead of modulating overall rates of RP gene transcription or cell growth, the nutrient-responsive phosphorylation of *Ifh1p* plays a more prominent role in the regulation of cellular replicative lifespan.

## INTRODUCTION

In the budding yeast *Saccharomyces cerevisiae*, ribosome biogenesis is tightly linked to cell growth. The synthesis of new ribosomes involves transcription of rDNA, ribosomal protein (RP) genes, and genes encoding accessory factors for rRNA processing and ribosome assembly, collectively called ribosome biogenesis (ribi) genes (Zaman et al., 2008). In rapidly growing cells, the majority of cellular transcriptional activity is devoted to ribosome biogenesis (Warner, 1999). This energetically and resource-intensive process is also essential for cell-cycle entry, given that an increase in translational capacity is needed to attain a critical cell mass before commitment to division (Jorgensen and Tyers, 2004). Although ribosome biogenesis is known to be regulated by nutrient-sensing signal transduction pathways such as the target of rapamycin (TOR) and protein kinase A (PKA) pathways, the precise manner by which key nutritional

cues are relayed to the ribosome biogenesis machinery has not been fully elucidated (Zaman et al., 2008).

The transcription factor *Ifh1p* is an essential regulator of RP genes. This coactivator can be dynamically recruited to RP gene promoters in response to nutrient availability and interacts with other transcription factors such as *Fhl1p* and *Rap1p* (Martin et al., 2004; Rudra et al., 2005; Schwalder et al., 2004; Wade et al., 2004). *Ifh1p* also forms a complex with the rRNA processing factors *Rrp7p*, *Utp22p*, and casein kinases, which have been termed the CURI complex (Rudra et al., 2007). Hence, *Ifh1p* might also regulate rRNA processing.

In this study, we utilized the yeast metabolic cycle (YMC) system to investigate the dynamics of ribosome biogenesis at high temporal resolution. Yeast cells become highly synchronized and undergo robust oscillations in oxygen consumption during continuous, glucose-limited growth (Figure 1A). These metabolic cycles have revealed the changes in gene expression and metabolism that occur as cells transition between different growth states (Tu et al., 2005; Tu et al., 2007). Each YMC is composed of three phases: oxidative (OX), reductive building (RB), and reductive charging (RC) (Figure 1A). The OX phase is characterized by increased mitochondrial respiration and rapid induction of growth genes. Genes involved in ribosome biogenesis (RP and ribi genes) are almost exclusively expressed during this phase (Cai et al., 2011). As oxygen consumption decreases, cells enter the RB phase and turn on cell-cycle genes as they begin division. In the RC phase, cells express many stress- and stationary-phase-associated genes and become quiescent-like (Shi et al., 2010). By sampling cycling cells as they synchronously transition between these different phases, we identified dynamic posttranslational modifications of *Ifh1p* and subsequently characterized their contributions to the regulation of ribosomal gene transcription, cell growth, and replicative lifespan.

## RESULTS

### In Addition to Ribosomal Subunit Genes, Several Translation Factors and Metabolic Genes Are Targets of *Ifh1p*

As previously characterized in the YMC, RP gene expression is induced robustly in the OX growth phase (Tu et al., 2005). The

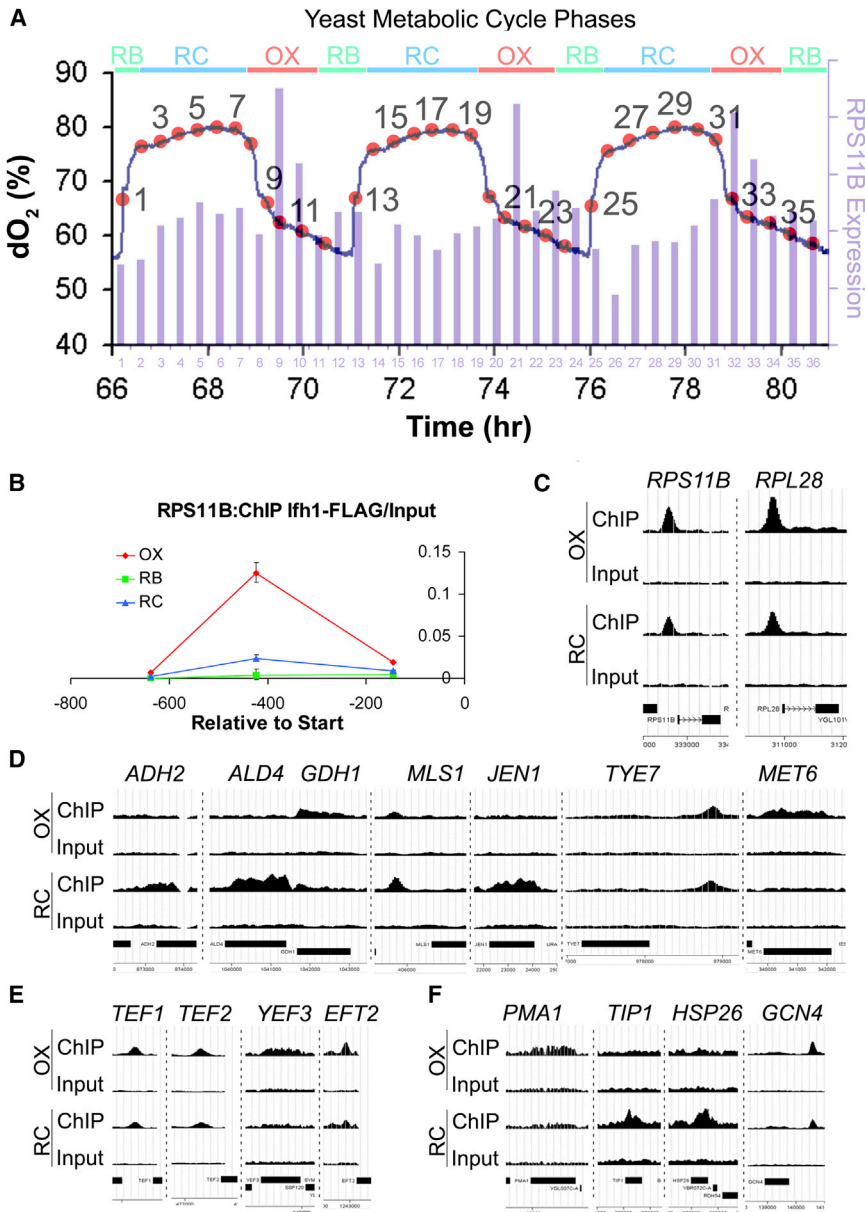


**Figure 1. Lfh1p Dynamically Binds to Ribosomal Subunit Genes during Growth**

(A) RP subunit genes are robustly induced during OX phase, which is the growth phase of the YMC. Shown is the expression profile of a representative RP gene *RPS11B* over three consecutive metabolic cycles (Tu et al., 2005).

(B) Lfh1p preferentially binds to RP genes during OX phase. Cells from representative time points at OX, RB, and RC phases were collected and fixed for ChIP-PCR. Three primer sets spanning the promoter region of *RPS11B* were used in the analysis of Lfh1p binding. Error bars come from technical triplicates.

(C) ChIP-seq reveals increased binding of Lfh1p to RP genes during growth. Genome-wide occupancy profile of Lfh1-FLAG was obtained for cells collected from OX (growth) and RC (G0/quiescent-like) phase of the YMC. Lfh1p binds to regulatory regions of nearly all RP genes. Data for two representative RP genes are shown with CisGenome.

(D) Lfh1p binds to non-RP genes, including genes involved in metabolism. The ChIP-seq data were scrutinized visually in order to identify all putative targets. Non-RP genes, including several involved in metabolism, are also targets of Lfh1p. Many of these genes have Lfh1p bound across the open reading frame instead of at the promoter.

(E) Lfh1p binds to genes encoding translation elongation factors.

(F) Lfh1p binds to other non-RP genes, including *GCN4*.

See also Figures S1 and S2.

association of Lfh1p at the promoters of RP genes is sensitive to growth conditions in batch culture (Schawalder et al., 2004; Wade et al., 2004). We tested whether Lfh1p binding at RP gene promoters is dynamic, given that a function of changes in the metabolic state experienced by cells during the YMC. Chromatin immunoprecipitation (ChIP) analysis confirmed that Lfh1p exhibited increased binding to a RP gene promoter (*RPS11B*) in the OX growth phase when massive RP gene transcription takes place (Figures 1A and 1B). To investigate how Lfh1p occupancy changes on a genome-wide scale, we conducted ChIP sequencing (ChIP-seq) experiments with cells collected from the OX, growth phase, and RC, quiescent-like phase. Peaks called by CisGenome from OX phase data are listed in Table S1. The

majority of Lfh1p targets are RP genes, which is in agreement with previous findings (Wade et al., 2004). Moreover, Lfh1p binding to RP genes was more apparent in OX than RC phase (Figure 1C), consistent with the ChIP-PCR data (Figure 1B). We also manually inspected the ChIP-seq data to identify putative targets that might have eluded peak-calling algorithms. Examination of all 137 RP genes revealed Lfh1p binding to proximal genomic regions of every RP gene except *RPS28A*, *RPL4A*, *RPL4B*, *RPL1A*, and *RPL18B*. Interestingly, Lfh1p also displayed binding to several non-RP genes, including metabolic genes (Figure 1D), translation factors (Figure 1E), and others such as *GCN4*, a transcription factor regulating amino acid biosynthetic genes (Figure 1F). Some additional peaks with weak signals are shown (Figure S1). Unlike peaks at RP genes, which are always at intergenic regions, some of the peaks at non-RP genes span the entire open reading frame. Moreover, the timing of Lfh1p binding often corresponded to the timing of the target's expression (Figure S2). These data indicate that, in addition to RP genes, Lfh1p regulates additional targets that are important for cell growth and metabolism.

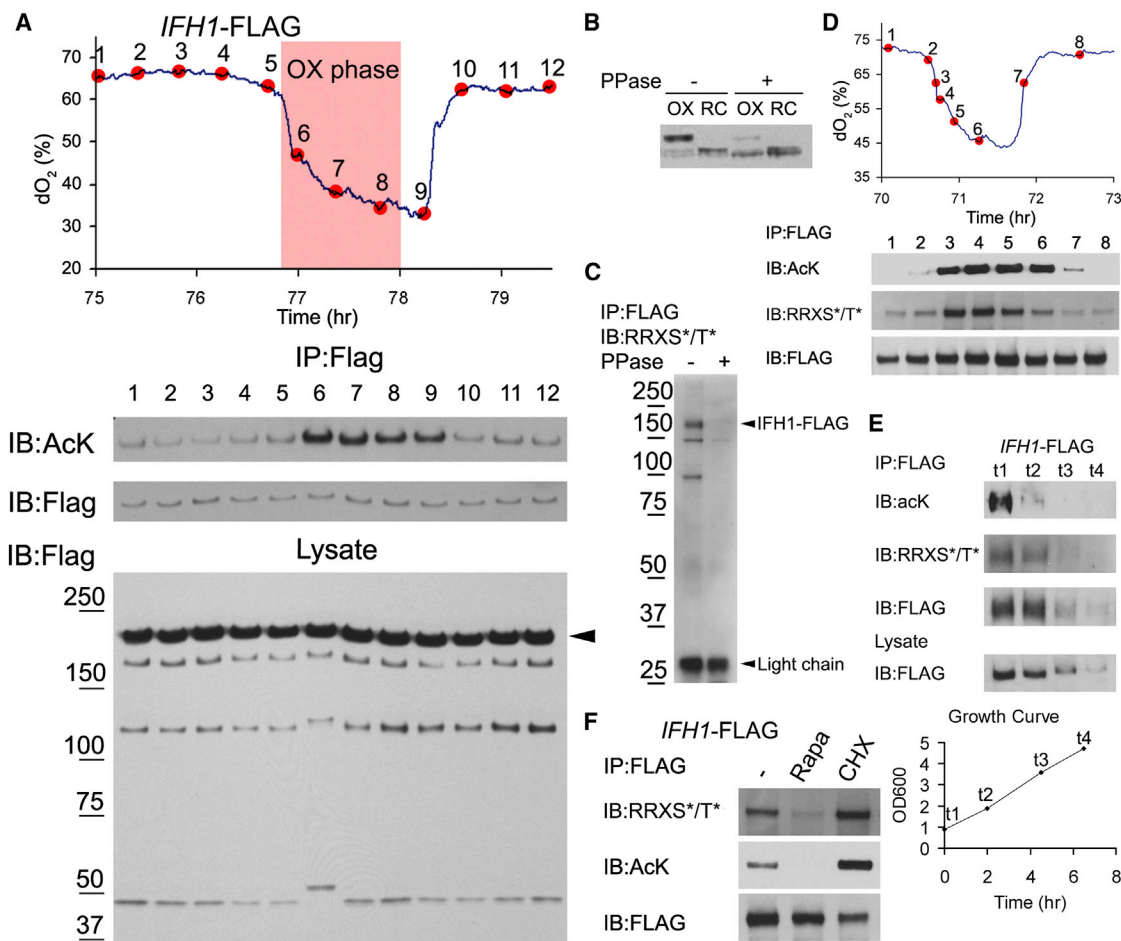


**Figure 2. Ifh1p Is Dynamically Acetylated and Phosphorylated During Growth**

(A) Ifh1p is dynamically acetylated and phosphorylated. Ifh1-FLAG was immunoprecipitated from cells collected across 12 time points of the YMC. Ifh1p is acetylated during the OX growth phase precisely when acetyl-CoA levels increase. A mobility shift of both the full-length Ifh1-FLAG protein (arrow) and its cleavage products was observed at time point 6, which is suggestive of phosphorylation.

(B) Ifh1p is phosphorylated. Lysates were prepared from OX and RC phase and treated with or without phosphatase (PPase). A cleavage product of Ifh1p at ~50 KDa is shown. The upshifted band in the OX phase sample was reduced after PPase treatment, indicating the shift was due to phosphorylation.

(C) Phosphorylated Ifh1p is recognized by a PKA substrate-specific antibody. An antibody that recognizes the phospho-PKA substrate motif RRXS\*/T\* (\* denotes phosphorylation) was used for immunoblotting against Ifh1p. The signal was eliminated after PPase treatment.

(D) Dynamic phosphorylation of Ifh1p. Both acetylation and phosphorylation of Ifh1p increase during the OX, growth phase.

(E) Acetylation of Ifh1p is sensitive to growth state. *IFH1*-FLAG cells were cultured in SD medium to log phase, and time points were collected as the cells were grown to a higher OD approaching stationary phase. Note that Ifh1p becomes deacetylated prior to the decrease in its protein level.

(F) The acetylation and phosphorylation of Ifh1p are regulated by TORC1. Cells were grown in YPD to log phase, and treated as indicated for 15 min. Phosphorylation and acetylation were both inhibited by rapamycin and stimulated by cycloheximide.

### Ifh1p Is Dynamically Acetylated and Phosphorylated During Growth Phase

We previously reported that acetyl-CoA, a central metabolite of carbon sources, drives the cellular transcriptional growth program by inducing the acetylation of histones present at growth genes and the G1 cyclin *CLN3* (Cai et al., 2011; Shi and Tu, 2013). This regulatory mechanism was discovered through a proteomic screen that identified dynamically acetylated components of the complex Spt-Ada-Gcn5-acetyltransferase (SAGA) (Cai et al., 2011). In subsequent validation of candidates, this screen also revealed Ifh1p to be a dynamically acetylated, nonhistone protein.

Ifh1p is acetylated precisely in tune with the increase in acetyl-CoA levels that accompanies entry into the OX growth phase (Figure 2A). This acetylation of Ifh1p mirrors that of SAGA and histones, occurring during the same temporal window of the YMC (Cai et al., 2011). Besides dynamic acetylation, we also observed a mobility shift of the full-length Ifh1-FLAG protein as well as its degradation products at a single time point in the midst of OX phase (Figure 2A) when RP genes are induced. The upshifted band in OX phase was reduced to the same size as the band in RC phase after treatment with phosphatase, indicating that the band shift was due to phosphorylation (Figure 2B). Given that the target of rapamycin complex 1 (TORC1) effectors

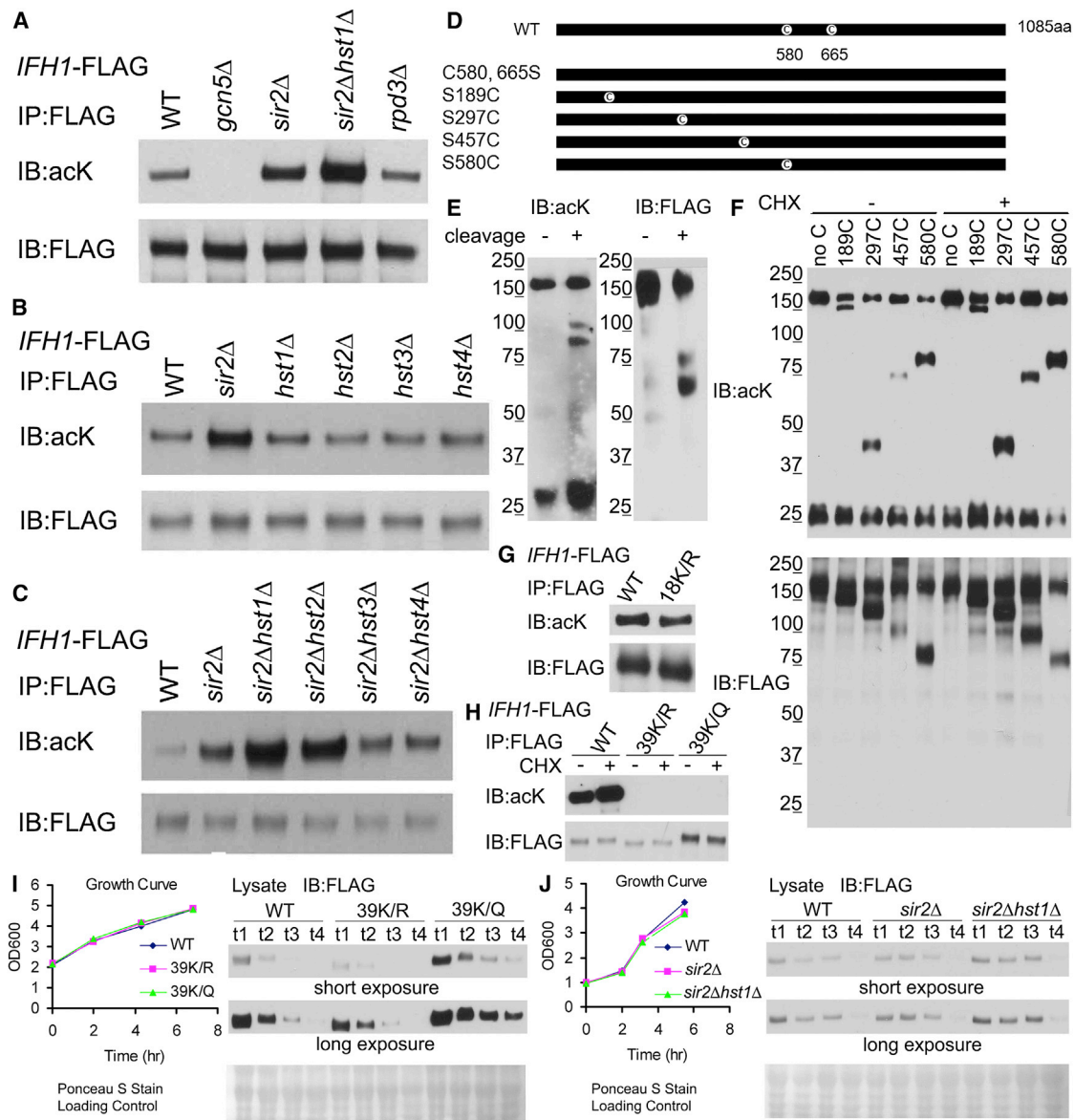


**Figure 3. Ifh1p Is Acetylated by Gcn5p and Deacetylated by Sirtuins**

(A) Ifh1-FLAG is acetylated by Gcn5p and deacetylated by Sir2p. Ifh1-FLAG was immunoprecipitated from YPD log phase cells from the indicated strains and probed with an acK antibody. Acetylation was abolished in a *gcn5Δ* strain and increased in *sir2Δ*, but not *rpd3Δ*, strains. Acetylation was further increased in a *sir2Δhst1Δ* strain.

(B) Ifh1p is deacetylated primarily by Sir2p. Ifh1p acetylation was compared in single-deletion mutants of the SIR2 family.

(C) Ifh1p is deacetylated by Hst1p and Hst2p in the absence of Sir2p. Ifh1p acetylation was compared in double-deletion mutants combining *sir2Δ* with deletions in *HST* genes.

(D) Schematic diagram for cysteine substitution mutants of Ifh1p used for mapping modification sites. Wild-type Ifh1p contains two cysteines. Mutations of C580 and C665 to serine were introduced. Serine-to-cysteine mutations were introduced at the indicated positions. See also Figure S3.

(E) Cleavage of the native form of Ifh1p suggests that acetylation sites are N-terminal to C580. Wild-type Ifh1p was immunoprecipitated from YPD log phase cultures and subjected to cleavage at cyanylated cysteines. The bands recognized by acK antibody and FLAG antibody are different sizes, suggesting that acetylation sites are not at fragments C-terminal to the cleavage sites, which are recognized by the FLAG antibody.

(F) The aa 189–297 region of Ifh1p contains acetylation sites. On the basis of a similar logic, it can be deduced that Ifh1p is acetylated between residues 189–297. Cycloheximide (CHX), which stimulates TORC1 signaling, generates the same pattern as the nontreated group.

(G) Mutation of 18 lysines in the aa 189–297 region only slightly decreased the acetylation of Ifh1p. K to R mutations were introduced in order to eliminate the lysines that can be acetylated in the above mapped region. Although acetylation was decreased, Ifh1p is still significantly acetylated.

(H) Mutation of 39 lysines in the aa 1–297 region eliminates the acetylation of Ifh1p. An additional 21 lysines before S189 were mutated, eliminating the residual acetylation on Ifh1p. CHX treatment did not result in any observable acetylation of this Ifh1p 39K/R mutant.

(legend continued on next page)



Sch9p and PKA have been linked to the ribosome biogenesis program (Zaman et al., 2008) and the substrate motif for these kinases is known to be RRXS/T, we tested whether the phosphorylation of Iffh1p could be detected by an antibody that specifically recognizes the phosphorylated serine or threonine in RRXS/T motifs (Figure 2C). This antibody recognized the phosphorylated form of Iffh1p but did not recognize it after phosphatase treatment, confirming that it is likely a substrate of this family of kinases. Then, we verified that Iffh1p is dynamically phosphorylated in the YMC specifically during the OX growth phase when ribosomal genes are activated (Figure 2D). Thus, using the YMC, we observed that Iffh1p is subjected to both acetylation and phosphorylation modifications, which specifically occur during growth phase.

### Posttranslational Modifications of Iffh1p Are Sensitive to Nutrient Cues and Regulated by TORC1

Then, we investigated these dynamic modifications on Iffh1p under typical batch culture conditions. In synthetic dextrose (SD) minimal medium, protein levels of Iffh1p decreased substantially as cells entered the stationary phase (Figure 2E). However, the acetylation of Iffh1p began to decrease prior to the decrease in Iffh1p protein levels, consistent with the idea that this modification is sensitive to nutrient state (Figure 2E). Given that TORC1 signaling has been shown to play key roles in nutrient sensing and ribosome biogenesis (Martin et al., 2004; Zaman et al., 2008), we tested whether posttranslational modifications of Iffh1p might be regulated by TORC1. To modulate TORC1 signaling, we used either rapamycin to inhibit TORC1 activity or cycloheximide, a translation elongation inhibitor that has been reported to stimulate TORC1 signaling (Huber et al., 2009). We observed that both the acetylation and phosphorylation of Iffh1p were strongly inhibited by rapamycin treatment. In contrast, these modifications were stimulated by cycloheximide (Figure 2F). Altogether, these data indicate that TORC1 can regulate the dynamic acetylation and phosphorylation of Iffh1p.

### Iffh1p Is Acetylated in Its N-Terminal Region by Gcn5p and Deacetylated by Sirtuins

Substrates of Gcn5p-containing SAGA appear to be dynamically acetylated in tune with intracellular acetyl-CoA fluctuations (Cai et al., 2011). Therefore, we suspected that the Gcn5p acetyltransferase might also catalyze the acetylation of Iffh1p. We confirmed that Iffh1p was no longer acetylated in strains lacking Gcn5p (Figure 3A). Then, we deleted several candidate deacetylases to determine which of them might regulate Iffh1p acetylation. Surprisingly, Rpd3p, the histone deacetylase known to regulate the transcription of RP and ribi genes (Huber et al., 2011) and the opening of rDNA repeats (Sandmeier et al., 2002), was not responsible for Iffh1p deacetylation. Instead, the deletion of the NAD<sup>+</sup>-dependent deacetylase *SIR2* resulted in

the increased acetylation of Iffh1p (Figure 3A). Deletion of *HST1*, the closest *SIR2* homolog, in combination with *sir2Δ* further increased Iffh1p acetylation, suggesting that these deacetylases are primarily responsible for Iffh1p deacetylation (Figure 3A). To further clarify the contribution of *SIR2* as well as the *HST* genes, we compared single deletion mutants as well as double deletion mutants combining *SIR2* deletion with different *HST* gene deletions. These data indicate that Sir2p is the primary deacetylase for Iffh1p. However, in the absence of Sir2p, Hst1p and Hst2p can also contribute to the deacetylation of Iffh1p (Figures 3B and 3C). Thus, Iffh1p is a significant nonhistone substrate of sirtuins in budding yeast.

Next, we mapped the acetylation sites on Iffh1p. The amino acid sequence composition of Iffh1p contains many clusters of basic and acidic residues that impose difficulty for proteomic analysis (Figure S3). Therefore, we sought an alternative approach by inducing peptide cleavage at cysteine residues after cyanylation (Tu and Wang, 1999). Fortunately, Iffh1p contains only two endogenous cysteine residues (Figure 3D), and mutating them to serine did not affect cell growth. We performed the mapping experiments with C-terminally FLAG-tagged Iffh1p immunoprecipitated from cells grown to log phase, conditions under which the protein is heavily acetylated. When the wild-type protein was cleaved at C580 and C665, peptide fragments C-terminal to the cleavage sites were recognized by a FLAG antibody. However, they ran at different sizes in comparison to the peptides recognized by an acetyl-lysine (ackK) antibody, suggesting that the acetylated sites are N-terminal to C580 (Figure 3E).

In a C580S/C665S Iffh1p mutant strain background, serine-to-cysteine mutations were introduced at various sites before residue 580 in order to induce peptide cleavage. The pattern of peptides recognized by FLAG antibody was compared to those recognized by ackK antibody in order to deduce the acetylated region within Iffh1p. To map additional sites possibly acetylated upon cycloheximide treatment (Figure 2F), we also included a set of cycloheximide-treated cells in the experiment. The peptides generated by cleavage at amino acid (aa) 189 were the same size in both blots, whereas peptides generated by cleavage at aa 297 were different sizes. Thus, the acetylated sites were most likely present between aa 189 and aa 297 (Figure 3F). However, mutating the 18 lysines within this region to arginine decreased but did not abolish acetylation of Iffh1p, indicating that there are additional lysines that can be modified (Figure 3G).

It remained possible that the cleavage fragment N-terminal to aa 189 was also acetylated but masked by the light chain after SDS-PAGE and western analysis. We mutated 21 additional lysine residues to arginine between aa 1–189. This mutant exhibited no detectable acetylation signal with or without cycloheximide treatment (Figure 3H). The K/Q acetylated mimic mutant was also made (Figure 3H). Although 39 lysines in this essential

(I) The Iffh1p 39K/Q acetylated mimic mutant is more stable during nutrient depletion. Lysates were prepared from the indicated strains at the indicated time points on the growth curve. Iffh1p levels decrease as cells grow to a higher density approaching stationary phase. Levels of Iffh1p are lower in K/R mutant and higher in K/Q mutant. The membrane was stained by Ponceau S and shown as a loading control. Two different exposures of the same blot are shown.

(J) *sir2Δ* and *sir2Δhst1Δ* mutants exhibit increased Iffh1p stability. Experiments were performed as described above with *sir2Δ* and *sir2Δhst1Δ* strains. Iffh1p seems to be more stable in the mutants where it is highly acetylated. Two different exposures of the same blot are shown. See also Figure S4.

protein were mutated, no obvious growth phenotypes were observed when either the 39K/R or 39K/Q mutants were tested under a variety of conditions (Figure S4A).

We observed that the acetylation of Ifh1p decreased prior to a decrease in its protein levels as cells entered stationary phase (Figure 2E), suggesting that acetylation regulates its protein stability and half-life. To measure the stability of Ifh1p, we avoided using protein synthesis inhibitors such as cycloheximide because they can induce TORC1 signaling and the acetylation of Ifh1p (Figure 2F), thereby confounding interpretation of the results. Instead, we measured Ifh1p levels in cells growing from a low to high density in SD medium. Lower levels of Ifh1p were detected in the acetylation-defective 39K/R mutant, whereas higher levels of Ifh1p were detected in the acetylated mimic 39K/Q mutant despite there being no differences in growth rate (Figure 3I). Consistent with these findings, sir2in deletion mutants that harbor increased acetylated Ifh1p also exhibited increased protein levels of Ifh1p, supporting the idea that Ifh1p stability is regulated by nutrient-responsive acetylation in its N-terminal region (Figure 3J).

Then, we tested whether the 39K/R and 39K/Q mutants resulted in any phenotypes related to growth or ribosomal gene transcription. The expression of RP genes, induction of RP genes in response to acetyl-CoA, and recruitment of Ifh1p to RP genes were not compromised in these mutants (Figures S4D and S4F). We also checked the expression of several non-RP Ifh1p target genes identified from the ChIP-seq experiment (Figure 1), but their levels remained similar in mutants in comparison to wild-type (WT) cells (Figure S4G). Moreover, these mutants exhibited similar growth and regrowth rates on a variety of carbon sources (Figures S4A and S4E) as well as chronological lifespan (Figure S4B). Thus, despite the effects on Ifh1p stability, we did not observe any significant growth phenotype in acetylation site mutants of Ifh1p.

### Ifh1p Is Phosphorylated by PKA at S969

To map the phosphorylation sites on Ifh1p, we used the same set of cysteine substitution mutants to deduce the general region of phosphorylation after peptide cleavage. The pattern of peptides recognized by both the FLAG antibody and phospho-PKA substrate antibody matched very well, suggesting that the phosphorylation site(s) lie C-terminal to C580 (Figure 4A). Then, we searched the C-terminal sequence of Ifh1p for PKA phosphorylation motifs (RRXS/T) and constructed single S/A or T/A mutants for each of the five sites that were identified. One single mutation converting S969 to A was sufficient to eliminate the signal recognized by the phospho-PKA substrate antibody (Figure 4B). Using this phosphorylation mutant and the acetylation mutants described above, we also observed that Ifh1p acetylation and phosphorylation modifications could occur independent of each other (Figure S4H).

Next, we tested whether S969 was phosphorylated by PKA using a *tpk1<sup>as</sup> tpk2<sup>as</sup> tpk3<sup>as</sup>* strain that expressed modified PKA alleles that are sensitive to the ATP analog 1NM-PP1 (Zaman et al., 2009). Upon treatment with 1NM-PP1, Ifh1p phosphorylation disappeared within 10 min, suggesting that it is indeed a PKA substrate (Figure 4C). Because Sch9p substrates share the same motif as PKA substrates, we also tested Ifh1p phos-

phorylation in a *sch9Δ* strain; however, no alteration of Ifh1p phosphorylation was observed (Figure S4I). These data show that PKA phosphorylates Ifh1p on S969 as cells enter growth.

To test the functional role of Ifh1p phosphorylation, we constructed S969A and S969D mutants and observed that they did not exhibit any obvious growth defects under a variety of nutrient conditions (Figure S4A). We also did not observe any significant phenotypes when subjecting these mutants to the same series of assays as the acetylation site mutants (Figures S4B–4G). Furthermore, mutation of acetylated sites in combination with the phosphorylated site also did not result in any substantial phenotype under the conditions tested.

### Nutrient-Responsive Posttranslational Modifications of Ifh1p Impact Replicative Lifespan

Interestingly, the posttranslational modifiers of Ifh1p—PKA, TORC1, and Sir2p—have each been implicated in the regulation of replicative lifespan (RLS) in budding yeast (Longo et al., 2012). Moreover, downstream targets of Ifh1p, such as RP subunits and *GCN4*, have also been linked to lifespan regulation (Steffen et al., 2008). Therefore, we tested whether mutations in the acetylated or phosphorylated sites of Ifh1p might also impact RLS. The acetylation site mutants of Ifh1p exhibited a modestly shorter RLS in comparison to the WT control. Notably, the single S969A mutant that cannot be phosphorylated exhibited a significantly increased RLS (30%–40%) (Figure 4D). However, the RLS of the S969D phosphomimetic mutant remained comparable to WT. Deletion of *GCN4*, which has been shown to be required for RLS extension triggered by 60S ribosomal subunit depletion (Steffen et al., 2008), did not affect RLS extension by the Ifh1p S/A mutant (Figure 4D). This modification of Ifh1p also did not affect *GCN4* expression levels (Figure S4G). Moreover, the S/A mutant was still able to extend RLS in a strain lacking *TOR1* (Figure 4D). However, the substantial RLS extension observed in the S/A mutant was entirely dependent on Sir2p (Figure 4D). The dependency on Sir2p is not surprising, given that the deletion of *SIR2* was observed to prevent lifespan extension in many long-lived yeast mutants (Delaney et al., 2011). Altogether, these data indicate that inhibiting the PKA-regulated phosphorylation of Ifh1p via mutation of a single site is sufficient to significantly increase RLS to an extent comparable to calorie restriction mimetic mutants (Kaeberlein et al., 2005). Thus, this nutrient-responsive phosphorylation modification on Ifh1p is involved in the regulation of cellular replicative potential as opposed to the regulation of rates of RP gene transcription.

## DISCUSSION

Although ribosome biogenesis is recognized as a key component of the cellular growth program, much remains unclear regarding how this fundamental process is coordinated with nutrient availability and metabolic state. In this study, we sampled highly synchronized cells across different growth states in the YMC to discover that an essential transcription factor, Ifh1p, involved in ribosomal gene transcription is subject to regulation by multiple nutrient-responsive, posttranslational modifications.

We also characterized the genome-wide occupancy of Ifh1p using the YMC. These ChIP-seq experiments provide a

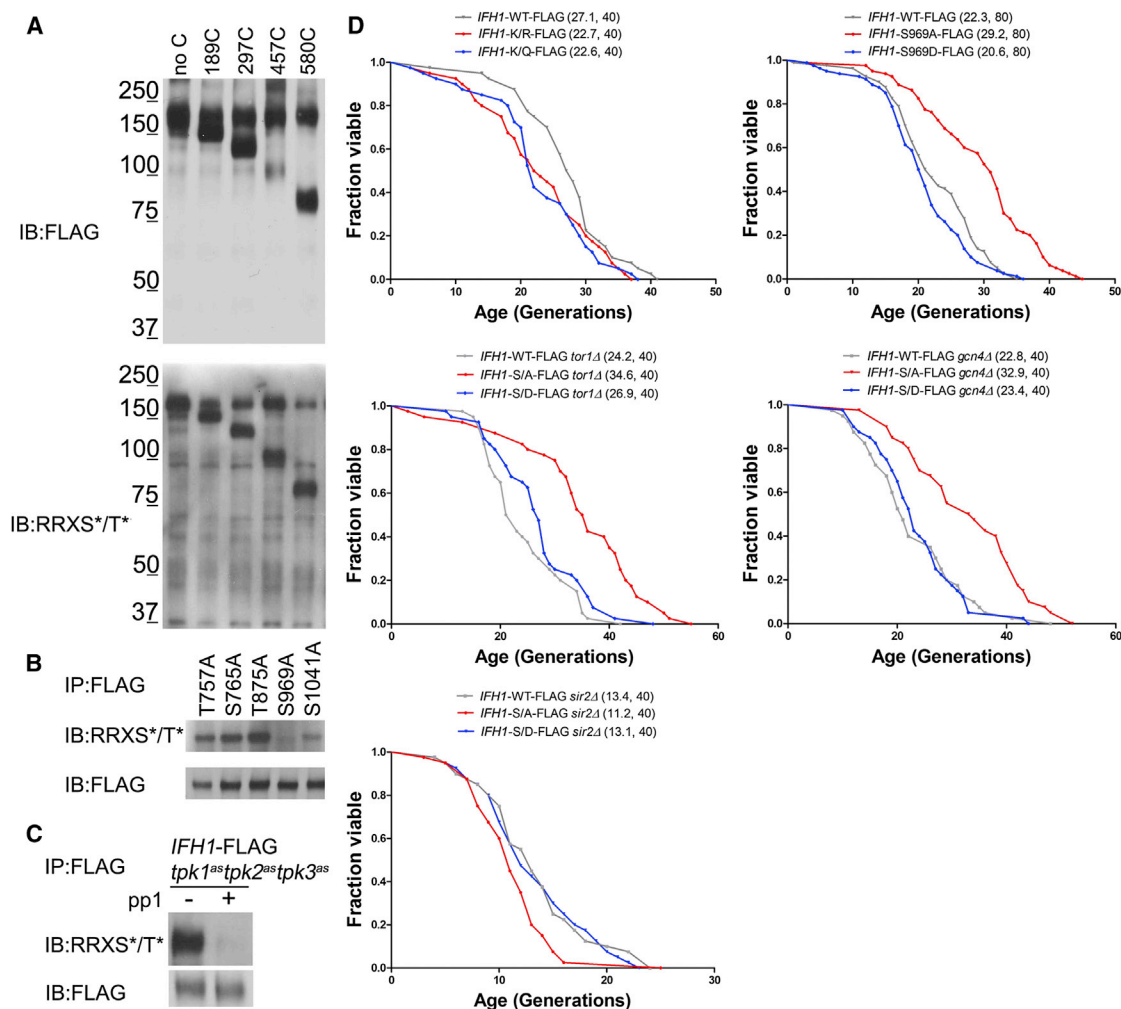


**Figure 4. Ifh1p Is Phosphorylated on S969 by PKA in Order to Regulate Replicative Lifespan**

(A) Ifh1p is phosphorylated at site(s) C-terminal of C580. On the basis of the mapping method described above, the exact match of FLAG and RRXS\*/T\* blotting patterns indicates the phosphorylated sites are after residue 580.

(B) Ifh1p is phosphorylated at S969. Candidate sites that match the motif RRXS\*/T\* were mutated to alanine. Mutation at S969 eliminated the signal recognized by the phospho-specific antibody.

(C) Ifh1p is phosphorylated by PKA. In an engineered strain (*tpk1<sup>as</sup>tpk2<sup>as</sup>tpk3<sup>as</sup>*) where PKA is rendered specifically sensitive to the inhibitor 1NM-PP1, phosphorylation of Ifh1p is eliminated within 10 min of treatment with 1NM-PP1.

(D) Nutrient-responsive phosphorylation of Ifh1p impacts RLS. The ~30%–40% increase in RLS of the S969A mutant was dependent on Sir2p, but not Gcn4p or Tor1p. Numbers in parentheses denote average lifespan and number of cells tested. Table S2 contains statistical analysis of the RLS data. See also Figure S4.

higher-resolution profile of Ifh1p occupancy in the genome and reveal additional important targets aside from RP genes. Several translation elongation factors were bound by Ifh1p, suggesting that their transcription may be regulated by Ifh1p. Moreover, *GCN4*, a transcriptional activator of amino acid biosynthetic genes (Hinnebusch, 2005), is also a target, suggesting that Ifh1p regulates the supply of amino acids for protein translation.

Ifh1p is dynamically acetylated by the Gcn5p-containing SAGA complex, specifically during growth. Gcn5p has the unique ability to acetylate its substrates in tune with acetyl-CoA levels (Cai et al., 2011), enabling the acetyltransferase to coordinate the acetylation of its targets in tune with the metabolic

state of a cell. Upon entry into growth, acetyl-CoA drives the acetylation of histones present at a set of over 1,000 growth genes, which include virtually all RP and ribi genes (Cai et al., 2011). The dynamic acetylation of Ifh1p coincides with the acetylation of histones and subunits within SAGA, suggesting that these substrates are all subjected to the same acetyl-CoA-regulated acetylation mechanism used to coordinate cell growth with this important intermediate in energy metabolism.

Ifh1p is rapidly deacetylated as cells transition out of the growth phase. Interestingly, the deacetylation of Ifh1p is catalyzed by NAD<sup>+</sup>-dependent sirtuins instead of non-NAD<sup>+</sup>-dependent deacetylases such as Rpd3p. When carbon sources

become limiting, acetyl-CoA levels decrease along with Gcn5p activity, and the activity of NAD<sup>+</sup>-dependent deacetylases may then predominate. Therefore, this transcriptional coactivator is subjected to a competition between acetyl-CoA-regulated acetylation and NAD<sup>+</sup>-dependent deacetylation that can be tipped in either direction by changes in metabolic state. Furthermore, our studies establish Lfh1p as a significant nonhistone substrate of Sir2p in yeast, and up to 39 lysine residues in its N-terminal region can be deacetylated.

Lfh1p is also dynamically phosphorylated by PKA. Both the phosphorylation and acetylation of Lfh1p are inhibited by rapamycin, suggesting that TORC1 is also a key regulator of Lfh1p. Previous studies implicated TORC1 and PKA signaling in the regulation of Crf1p, a repressor of RP gene transcription (Martin et al., 2004). TORC1 and PKA activation result in the dephosphorylation of Crf1p and its confinement to the cytosol. Upon the inactivation of TORC1, Crf1p becomes phosphorylated and nuclear, leading to the repression of RP genes. Furthermore, TORC1 and PKA inactivate repressors of ribi genes such as Dot6p and Tod6p (Huber et al., 2011; Lippman and Broach, 2009). Stb3p, a repressor of rRNA processing genes, is also inactivated by TORC1 and glucose (Huber et al., 2011; Liko et al., 2010). We show that Lfh1p is yet another ribosomal transcription factor that is exposed to phosphorylation by TORC1 and PKA signaling.

The consequences of mutations in the acetylated or phosphorylated sites in Lfh1p on cell growth appear extremely modest despite the fact that the protein is essential. We did not observe significant growth defects for the 39K/R, 39K/Q, S969A, or S969D mutants, nor did we find any differences in their ability to bind RP gene promoters or activate RP genes (Figure S4). Although the 39K/R mutant decreased the overall Lfh1p levels in the cell, there is apparently still sufficient Lfh1p to achieve normal levels of RP gene transcription. Lfh1p has a very peculiar protein sequence that contains many clusters of acidic and basic residues but lacks any defined domains (Figure S3). We predict that it acts as a scaffold in order to bring together numerous other factors for enabling the activation of RP genes. The dynamic modifications within Lfh1p might also be a consequence of its proximity to other macromolecules that are subjected to nutrient-responsive regulation (e.g., the acetyl-CoA-driven acetylation of histones at RP genes catalyzed by SAGA and the phosphorylation-dependent regulation of Crf1p localization by TORC1 and PKA). Moreover, cycloheximide treatment significantly increased both the phosphorylation and acetylation of Lfh1p, suggesting that these modifications stimulate Lfh1p and possibly other RP transcription factors under conditions of translation stress that could be frequently encountered in the wild in the face of unpredictable nutrient availability.

Finally, it is both interesting and unexpected that the nutrient-responsive phosphorylation of Lfh1p instead appears to function primarily in the regulation of replicative lifespan. A single mutation preventing Lfh1p phosphorylation was sufficient to extend RLS in a manner comparable to mutations in the TORC1-Sch9 and PKA signaling pathways that mimic caloric restriction. The fact that this Lfh1p modification specifically impacts RLS, but not apparent rates of RP gene transcription and cell growth, supports the existence of a specific cellular mechanism for weighing

replicative potential that is separable from the overall growth rate of the cell. Thus, future work will be required in order to decipher the specific mechanism by which the phosphorylation of this ribosomal gene transcription factor functions in response to nutrients to limit the replicative potential of yeast cells.

## EXPERIMENTAL PROCEDURES

### Antibodies

Anti-acetyl-lysine (ST1027, Calbiochem) and anti-phospho-PKA substrate (RRXS\*/T\*; 100G7E, Cell Signaling Technology) were used for the detection of acetylation and phosphorylation on Lfh1p. FLAG antibody (M2, Sigma-Aldrich) was used for western blotting, immunoprecipitation, and ChIP with *IFH1*-FLAG cells.

### Chromatin Immunoprecipitation

ChIP was performed according to a well-established protocol with minor modifications (Ezhkova and Tansey, 2006). Lysates were sonicated with a Bioruptor, precleared, and incubated with 2  $\mu$ g FLAG M2 antibody overnight. After washes, DNA was recovered and purified. Real-time PCR was performed in triplicate with SYBR green reagents (Applied Biosystems). PCR primers were designed with Primer Express (Applied Biosystems).

### ChIP-Seq

Library construction was performed using a protocol from the following website: [http://bioinfo.mbb.yale.edu/array/Solexa\\_LibraryPrep\\_20080229ge.pdf](http://bioinfo.mbb.yale.edu/array/Solexa_LibraryPrep_20080229ge.pdf). Sequencing was performed on an Illumina GA IIX supervised by the University of Texas Southwestern Microarray Core Facility. The data were assembled to the reference genome by Bowtie and analyzed by CisGenome as described in its online tutorial (Ji et al., 2008). Peaks were annotated with the gene whose transcription start site is closest to the peak region. CisGenome was used to visualize ChIP-seq peaks.

### Yeast Strains and Methods

Deletion strains and tagged strains were made by homologous recombination followed by drug selection (Longtine et al., 1998). Site-directed mutagenesis was performed by PCR in which primers containing the mutation were used to generate two PCR fragments that contain  $\sim$ 45 bp overlapping regions containing the mutation. Fusion PCR was performed to anneal two fragments together, and the product was used for transformation. Synthesized templates were used for constructing 18K/R, 39K/R, and 39K/Q mutants. All strains are listed in Table S3. The CEN.PK background was used in most experiments except for the RLS assays.

### Yeast Cell Lysis and Immunoprecipitation

Typically,  $\sim$ 100 OD yeast cells were lysed in 1 ml lysis buffer (100 mM Tris-Cl [pH 7.5], 100 mM NaCl, 50 mM NaF, 1 mM EDTA, 1 mM EGTA, 0.1% Tween-20, 10% glycerol, 50 mM sodium butyrate, 50 mM nicotinamide, 5  $\mu$ M trichostatin A, 1 mM PMSF, 10  $\mu$ M leupeptin, 5  $\mu$ M pepstatin A, Roche protease inhibitor cocktail, and 14 mM  $\beta$ -mercaptoethanol) by bead beating, and immunoprecipitation was performed by incubating the lysate with 15  $\mu$ l magnetic beads (Invitrogen) conjugated to 2  $\mu$ g FLAG M2 antibody (Sigma-Aldrich). After being washed three times in the same buffer, the beads were boiled in order to release the precipitated proteins for western blot analysis.

### Mapping by Cleavage at Cyanylated Cysteines

Immunoprecipitated Lfh1p bound to magnetic beads was resuspended in reaction buffer (0.1 M Tris acetate [pH 8.0] and 8 M GnCl). Then, 2-nitro-5-thiocyanobenzoic acid was added to 1 mM, and the reaction was incubated at room temperature for 30 min. Sodium hydroxide was added in order to adjust the pH to 9.0, and the reaction was incubated at 37°C overnight. The reaction was boiled and run on a 3%–8% Tris acetate precast gel.

### Lifespan Assays

RLS assays were carried out as described previously (Steffen et al., 2009). Unless otherwise noted, all lifespan experiments were performed on yeast



extract-peptone-dextrose growth medium plates with 2% glucose. The BY strain background was used for RLS assays.

### ACCESSION NUMBERS

The wig files for the ChIP-seq tracks shown in Figure 1 have been deposited into the NCBI Gene Expression Omnibus and are available at accession number GSE39147.

### SUPPLEMENTAL INFORMATION

Supplemental Information includes four figures and three tables and can be found with this article online at <http://dx.doi.org/10.1016/j.celrep.2013.08.016>.

### ACKNOWLEDGMENTS

We thank Dan Gottschling for strains and helpful discussions, Erin O'Shea for the *tpk-as* strains, and Kevan Shokat for the 1NM-PP1 inhibitor. This work was supported by award R01GM094314 from the National Institute of General Medical Sciences (B.P.T.), award R01AG033373 from the National Institute of Aging (B.K.K.), the University of Texas Southwestern Endowed Scholars Program (B.P.T.), a Packard Fellowship (B.P.T.), and a Frank and Sara McKnight Graduate Fellowship (L.C.). B.P.T. is a consultant and B.P.T. and L.C. are shareholders of Peloton Therapeutics.

Received: September 5, 2012

Revised: July 29, 2013

Accepted: August 8, 2013

Published: September 12, 2013

### REFERENCES

- Cai, L., Sutter, B.M., Li, B., and Tu, B.P. (2011). Acetyl-CoA induces cell growth and proliferation by promoting the acetylation of histones at growth genes. *Mol. Cell* 42, 426–437.
- Delaney, J.R., Sutphin, G.L., Dulken, B., Sim, S., Kim, J.R., Robison, B., Schleit, J., Murakami, C.J., Carr, D., An, E.H., et al. (2011). Sir2 deletion prevents lifespan extension in 32 long-lived mutants. *Aging Cell* 10, 1089–1091.
- Ezhkova, E., and Tansey, W.P. (2006). Chromatin immunoprecipitation to study protein-DNA interactions in budding yeast. *Methods Mol. Biol.* 313, 225–244.
- Hinnebusch, A.G. (2005). Translational regulation of GCN4 and the general amino acid control of yeast. *Annu. Rev. Microbiol.* 59, 407–450.
- Huber, A., Bodenmiller, B., Uotila, A., Stahl, M., Wanka, S., Gerrits, B., Aebersold, R., and Loewith, R. (2009). Characterization of the rapamycin-sensitive phosphoproteome reveals that Sch9 is a central coordinator of protein synthesis. *Genes Dev.* 23, 1929–1943.
- Huber, A., French, S.L., Tekotte, H., Yerlikaya, S., Stahl, M., Perepelkina, M.P., Tyers, M., Rougemont, J., Beyer, A.L., and Loewith, R. (2011). Sch9 regulates ribosome biogenesis via Stb3, Dot6 and Tod6 and the histone deacetylase complex RPD3L. *EMBO J.* 30, 3052–3064.
- Ji, H., Jiang, H., Ma, W., Johnson, D.S., Myers, R.M., and Wong, W.H. (2008). An integrated software system for analyzing ChIP-chip and ChIP-seq data. *Nat. Biotechnol.* 26, 1293–1300.
- Jorgensen, P., and Tyers, M. (2004). How cells coordinate growth and division. *Curr. Biol.* 14, R1014–R1027.
- Kaeberlein, M., Powers, R.W., 3rd, Steffen, K.K., Westman, E.A., Hu, D., Dang, N., Kerr, E.O., Kirkland, K.T., Fields, S., and Kennedy, B.K. (2005). Regulation of yeast replicative life span by TOR and Sch9 in response to nutrients. *Science* 310, 1193–1196.
- Liko, D., Conway, M.K., Grunwald, D.S., and Heideman, W. (2010). Stb3 plays a role in the glucose-induced transition from quiescence to growth in *Saccharomyces cerevisiae*. *Genetics* 185, 797–810.
- Lippman, S.I., and Broach, J.R. (2009). Protein kinase A and TORC1 activate genes for ribosomal biogenesis by inactivating repressors encoded by Dot6 and its homolog Tod6. *Proc. Natl. Acad. Sci. USA* 106, 19928–19933.
- Longo, V.D., Shadel, G.S., Kaeberlein, M., and Kennedy, B. (2012). Replicative and chronological aging in *Saccharomyces cerevisiae*. *Cell Metab.* 16, 18–31.
- Longtine, M.S., McKenzie, A., 3rd, Demarini, D.J., Shah, N.G., Wach, A., Brachat, A., Philippsen, P., and Pringle, J.R. (1998). Additional modules for versatile and economical PCR-based gene deletion and modification in *Saccharomyces cerevisiae*. *Yeast* 14, 953–961.
- Martin, D.E., Soulard, A., and Hall, M.N. (2004). TOR regulates ribosomal protein gene expression via PKA and the Forkhead transcription factor FHL1. *Cell* 119, 969–979.
- Rudra, D., Zhao, Y., and Warner, J.R. (2005). Central role of Ifh1p-Fhl1p interaction in the synthesis of yeast ribosomal proteins. *EMBO J.* 24, 533–542.
- Rudra, D., Mallick, J., Zhao, Y., and Warner, J.R. (2007). Potential interface between ribosomal protein production and pre-rRNA processing. *Mol. Cell Biol.* 27, 4815–4824.
- Sandmeier, J.J., French, S., Osheim, Y., Cheung, W.L., Gallo, C.M., Beyer, A.L., and Smith, J.S. (2002). RPD3 is required for the inactivation of yeast ribosomal DNA genes in stationary phase. *EMBO J.* 21, 4959–4968.
- Schawaldner, S.B., Kabani, M., Howald, I., Choudhury, U., Werner, M., and Shore, D. (2004). Growth-regulated recruitment of the essential yeast ribosomal protein gene activator Ifh1. *Nature* 432, 1058–1061.
- Shi, L., and Tu, B.P. (2013). Acetyl-CoA induces transcription of the key G1 cyclin CLN3 to promote entry into the cell division cycle in *Saccharomyces cerevisiae*. *Proc. Natl. Acad. Sci. USA* 110, 7318–7323.
- Shi, L., Sutter, B.M., Ye, X., and Tu, B.P. (2010). Trehalose is a key determinant of the quiescent metabolic state that fuels cell cycle progression upon return to growth. *Mol. Biol. Cell* 21, 1982–1990.
- Steffen, K.K., MacKay, V.L., Kerr, E.O., Tsuchiya, M., Hu, D., Fox, L.A., Dang, N., Johnston, E.D., Oakes, J.A., Tchao, B.N., et al. (2008). Yeast life span extension by depletion of 60s ribosomal subunits is mediated by Gcn4. *Cell* 133, 292–302.
- Steffen, K.K., Kennedy, B.K., and Kaeberlein, M. (2009). Measuring replicative life span in the budding yeast. *J. Vis. Exp.* 28, 1209.
- Tu, B.P., and Wang, J.C. (1999). Protein footprinting at cysteines: probing ATP-modulated contacts in cysteine-substitution mutants of yeast DNA topoisomerase II. *Proc. Natl. Acad. Sci. USA* 96, 4862–4867.
- Tu, B.P., Kudlicki, A., Rowicka, M., and McKnight, S.L. (2005). Logic of the yeast metabolic cycle: temporal compartmentalization of cellular processes. *Science* 310, 1152–1158.
- Tu, B.P., Mohler, R.E., Liu, J.C., Dombek, K.M., Young, E.T., Synovec, R.E., and McKnight, S.L. (2007). Cyclic changes in metabolic state during the life of a yeast cell. *Proc. Natl. Acad. Sci. USA* 104, 16886–16891.
- Wade, J.T., Hall, D.B., and Struhl, K. (2004). The transcription factor Ifh1 is a key regulator of yeast ribosomal protein genes. *Nature* 432, 1054–1058.
- Warner, J.R. (1999). The economics of ribosome biosynthesis in yeast. *Trends Biochem. Sci.* 24, 437–440.
- Zaman, S., Lippman, S.I., Zhao, X., and Broach, J.R. (2008). How *Saccharomyces* responds to nutrients. *Annu. Rev. Genet.* 42, 27–81.
- Zaman, S., Lippman, S.I., Schnepfer, L., Slonim, N., and Broach, J.R. (2009). Glucose regulates transcription in yeast through a network of signaling pathways. *Mol. Syst. Biol.* 5, 245.